

Coulomb Blockade in the Insulating Regime of Short Superconducting Nanowires

A. T. Bollinger*, A. Rogachev*, and A. Bezryadin

Department of Physics, University of Illinois at Urbana-Champaign, Urbana, Illinois 61801-3080, USA

(Dated: December 2, 2024)

Short thin wires made of a superconducting metal exhibit a zero-temperature superconductor to insulator transition (SIT) as their thickness is reduced. We report a detailed study of homogeneous MoGe nanowires that belong to the insulating phase of the SIT. Measurements of the conductance at various temperatures and at high voltage bias are well described by the theory of weak Coulomb blockade of coherent single-electron transport. This indicates that insulating-phase nanowires behave as normal metal conductors, with completely suppressed superconductivity. We also show that superconducting-phase wires exhibit excellent agreement with the theory of thermally activated phase slips, even in the vicinity of the SIT.

PACS numbers: 74.78.Na, 73.23.Hk, 74.50.+r

One of the fundamental unresolved problems concerning one-dimensional (1D) superconductivity is to understand the mechanism that drives the apparent superconductor-insulator transition (SIT) [1, 2, 3, 4, 5]. Under certain conditions, usually associated with some critical resistance per square [1], critical resistance [2], or critical diameter [5], a wire can lose its superconductivity and acquire some characteristics of insulating behavior, such as an increasing resistance with cooling and a zero-bias resistance peak [2, 3].

A number of models have been suggested which capture certain features of the SIT. Some models rely on the “fermionic” mechanism, in which the Coulomb interaction [6] drives the critical temperature, T_c , of the superconductor to zero, thus destroying superconductivity completely. In other, “bosonic”, models the order parameter magnitude remains above zero at the SIT critical point, but the coherence and thus the ability of the wire to carry a supercurrent is destroyed by quantum fluctuations such as quantum phase slips (QPS) [7, 8, 9, 10, 11]. In many models, the interaction of the superconductor with the Caldeira-Leggett environment is of crucial importance [8, 10, 11, 12, 13]. Conditions that make QPS observable in experiment and the relation of the QPS to the phase diagram of the SIT are still under debate [1, 2, 3, 4, 5, 14, 15].

Here, we report measurements on many samples with single nanowires, in the vicinity of the SIT. The focus of this Letter is on wires in the insulating phase, which are the least understood. We find that the behavior of these wires follows the predictions of theories considering the effect of Coulomb blockade (CB) of coherent transport in normal metal conductors [16, 17, 18]. These theories were recently used to interpret the electron transport in short Cu bridges [19]. Here, we also confirm that all wires in the superconducting phase, even those that are close to the SIT, obey the predictions of the theory of thermally activated phase slips (TAPS), due to Langer, Amblegaokar, McCumber, and Halperin (LAMH) [20]. This indicates that a true superconducting regime, with QPS

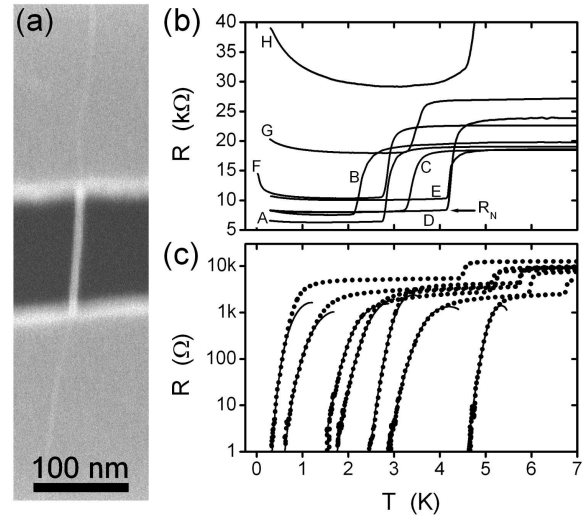


FIG. 1: (a) SEM micrograph of a ~ 8 nm wide nanowire (light) suspended over the trench in SiN. The white regions at the end of the wire indicate that the underlying nanotube is straight and the wire is rigidly suspended across the trench in SiN. Resistance vs. temperature curves for insulating and superconducting wires are shown in (b) and (c) respectively. The arrow in (b) shows our defibrillation of the normal resistance applied to the wire D. In (c), solid lines indicate fits to the LAMH theory.

fully suppressed (i.e. zero resistance at zero temperature) is realized in this group of wires.

The nanowires are fabricated by sputtering of amorphous $\text{Mo}_{79}\text{Ge}_{21}$ alloy on top of suspended fluorinated single-wall carbon nanotubes [2, 3, 14]. The length of our wires varies in the range 45-150 nm. The wires are homogeneous as is seen from the scanning electron microscopy (SEM) images [Fig. (1(a))]. The measurements are performed in ${}^4\text{He}$ and ${}^3\text{He}$ cryostats, and one sample (sample F) was measured in a dilution refrigerator.

Resistance vs. temperature data for representative insulating and superconducting samples are shown in Figs. 1(b) and (c), respectively. The transition observed

in all samples at higher temperatures is that of the film electrodes, which are measured *in series* with the wire. Resistance measured immediately after the film becomes superconducting is taken as the normal or high-temperature resistance of the wire, R_N . The nominal thicknesses of deposited MoGe varied in the interval 4.0–8.5 nm. Accordingly, the critical temperature of the thin film electrodes decreases as we go from the thickest superconducting samples to the thinnest insulating ones [Fig. 1 (b) and (c)]. In Fig. 1 (c) we see that the resistive transitions of the superconducting wires is well described by the LAMH theory of TAPS. For samples with the lowest T_c , we used, for the thermodynamic critical field in the LAMH free energy, an empirical expression $H_c(T) \propto 1 - (T/T_c)^2$ [21], instead of the usual $H_c(T) \propto 1 - T/T_c$. Good agreement with the LAMH theory confirms that the observed superconducting regime is a "true" superconducting phase, i.e. the wire resistance approaches zero in the limit of zero temperature.

The $R(T)$ curves of insulating wires show an upturn at the lowest temperatures, with R increasing as T decreases. No reentrant downturn was ever observed, even for sample F, which was measured down to 10 mK. One proposed explanation for the insulating behavior is that it is due to quantum phase slips. There are actually two ideas centered around QPS. The first is that the SIT is not a true quantum phase transition but rather a smooth crossover from a state in which the QPS rate is finite but too low to be detected to a state in which the QPS rate is so high that only quasiparticles contribute to the current [5, 9, 15]. In this approach the insulating behavior emerges because weak localization and electron-electron interaction corrections to normal wire resistance are divergent at low temperatures. We find, however, that the picture of the crossover is not consistent with our observations. None of our superconducting samples shows signs of greatly broadened resistive transitions [5] or of the resistance "tails" [7, 15], which are characteristics of the crossover. On the contrary, the measurement of the wires in high-bias regime revealed that the LAMH variation holds over eleven orders of magnitude in resistance [14]. The observed abrupt change from the LAMH to the insulating behavior strongly suggests that a quantum phase transition does occur in short nanowires. We speculate that this SIT takes place due to coupling of QPS to gapless excitations [8, 10, 11, 12] similar to the Chakravarty-Schmid transition in Josephson junctions [22]. Our results can be understood assuming that superconductivity is completely suppressed in the insulating-phase wires, possibly due to the proliferation of QPS.

To understand the increase in resistance for insulating samples we compare our data with the predictions of theories that consider the effects of the CB in diffusive conductors. Nazarov showed that the CB can survive in a structure where plates of a capacitor are connected by a homogeneous normal wire, even if its resistance is

much lower than the von Klitzing resistance quantum, $R_K = h/e^2$, provided the wire is short enough to act as a coherent scatter [16]. In other words, although a wire may be homogeneous and continuous, i.e. no breaks exist to act as tunnel barriers, the CB can still be present. Golubev and Zaikin (GZ) [17] extended the analysis to include a derivation of the $I(V)$ dependence, thus providing a clear means for comparison with experiment. Levy Yeyati *et al.* [18] established a link between the shot noise reduction and the CB for a conduction channel of arbitrary transmission. For a coherent scatter in weak CB regime the theory of Levy Yeyati *et al.* yields results equivalent to the GZ theory.

According to the GZ theory, at high temperatures ($k_B T > E_C = e^2/2C$, E_C is the charging energy) the zero-bias conductance, $G(T) \equiv 1/R(T)$, of a coherent scatter connecting the plates of a capacitor C is:

$$\frac{G(T)}{G_0} \simeq 1 - \beta \left[\frac{E_C}{3k_B T} - \left(\frac{3\zeta(3)}{2\pi^4} g + \frac{1}{15} \right) \left(\frac{E_C}{k_B T} \right)^2 \right] \quad (1)$$

where $\beta = 1/3$ for diffusive wires, which is our case, and $\beta = 1$ for tunnel junctions. Here $\zeta(3) \simeq 1.202$, $g \equiv G_0 R_K$ and G_0 is the conductance in the absence of the CB. Note that apart from the second order term in $E_C/k_B T$ this result is the same as the one obtained by Kaupinnen and Pekola for a single tunnel junction [23]. The GZ theory does not take into account the impedance of the environment, which is important since we have just one barrier (the wire itself), but not a Coulomb island with two barriers. The dynamical Coulomb blockade,

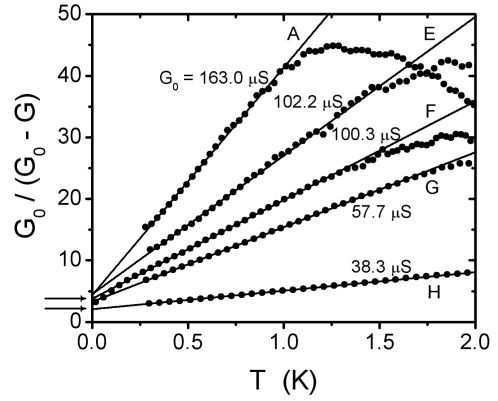


FIG. 2: Normalized and inverted conductance change vs. temperature for samples A, E, F, G, and H. The solid lines are fits to the GZ theory [Eq. (2)]. Values of the fitting parameter G_0 are indicated and the range of theoretical predictions for the $T = 0$ offsets is shown along the vertical axis by arrows. For these samples, $G_0^{-1} = 6.14, 9.78, 9.97, 17.33$, and $26.10 \text{ k}\Omega$ and $R_N = 6.43, 10.33, 10.50, 18.05$, and $32.46 \text{ k}\Omega$, respectively.

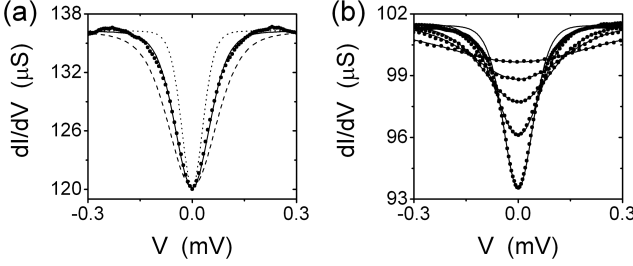


FIG. 3: (a) Differential conductance vs. bias voltage for sample B at $T = 0.28$ K. Comparisons to the GZ theory are shown with $q_{eff} = e$ (dashed line), $q_{eff} = 1.29e$ (solid line), and $q_{eff} = 2e$ (dotted line). (b) Differential conductance vs. bias voltage curves at different temperatures for sample E with $T = 0.3$ (deepest dip), 0.5 , 0.75 , 1.0 , and 1.5 K (shallowest dip). The same $q_{eff} = 1.5e$ was used to fit all data. Fits of similar quality were obtained for other samples.

relevant to this case, was considered by Joyez and Esteve [24]. In fact, for highly resistive tunnel junctions they found that at $E_C/k_B T \ll 1$ the conduction obeys the same Eq. (1), but with the value of parameter g defined differently: $g = R_K/R_{env}$ (R_{env} is the impedance of the environment).

By appropriate expansion in $E_C/k_B T$, Eq. (1) can be rewritten as a liner function of T :

$$\frac{G_0}{G_0 - G(T)} = \frac{3k_B T}{\beta E_C} + \frac{9}{\beta} \left(\frac{3\zeta(3)}{2\pi^4} g + \frac{1}{15} \right) \quad (2)$$

In Fig. (2) we replotted the $R(T)$ data according to Eq. 2. Parameter G_0 , adjusted to produce best linearity of curves, agrees well with the high-bias conductance, as expected. As indicated by Eq. 2, the offset at $T = 0$ is determined by parameter g . The arrows in Fig. 2 represent the expected range of the offsets when g is set by the wire resistance according to $g = R_K/R_N$. This range is in an agreement with the experiment. Our data agree equally well with the theory of Joyez and Esteve [24], if we assume that the resistance of the environment is set by the resistance of the nanowire, as was suggested in Ref. [25] for high-conductance tunnel junctions.

A thermally smeared zero-bias anomaly (ZBA) is observed in the $dI(V)/dV$ dependence of all our insulating-phase wires. Some examples are shown in Fig. 3. The shape of the dI/dV curves can be compared with the GZ theory, in which the CB anomaly in the $I(V)$ dependence is given as

$$I = V G_0 - \frac{e\beta k_B T}{\hbar} \text{Im} \left[w\Psi \left(1 + \frac{w}{2} \right) - iv\Psi \left(1 + \frac{iv}{2} \right) \right] \quad (3)$$

where $w = u + iv$, $u = gE_C/\pi^2 k_B T$, $v = eV/\pi k_B T$, and $\Psi(x)$ is the digamma function. The expression for

the fitting procedure was obtained by differentiating Eq. (3) and making a series expansion of $\Psi(x)$. Samples with high R_N agree well with the theory. For samples with relatively small R_N , the width of the experimentally observed dip was found to be *narrower* than the one predicted by the GZ theory [Fig. 3(a)]. This can not be explained by the presence of weak links in the wire or by Joule heating, since these factors would *broaden* the dip. One way to interpret these results is to assume that in addition to the single-electron transfer, a double-electron transfer by Andreev reflections is also occurring at the wire ends that are connected to the superconducting film electrodes. The detailed mechanism of the effect of the Coulomb blockade on the Andreev reflections may be quite complex. For a single channel point contact, Levy Yeyati *et al.* recently found that the environment produces a blockade of multiple Andreev reflection processes as if they would correspond to transmission of “shots” of charge ne [26]. The GZ theory does not include superconductivity of the leads. We however find empirically that the dI/dV obtained from Eq. (3) can be used to fit our data with e replaced by an effective charge q_{eff} , which we used as a fitting parameter along with G_0 and E_C . The differential conductance at various temperatures shows a good agreement with theory [Fig. 3(b)]. As shown in Figs. 4(a) and 4 (b), the values obtained from these fits for G_0 and E_C are close to those found from fits to the $G_0/(G_0 - G(T))$ vs. T data, thus confirming the consistency of our interpretation. Furthermore, it is clear from Fig. 4(a) that G_0 is very close to R_N^{-1} for all samples.

The charging energy extracted from the $G_0/(G_0 - G(T))$ vs. T dependence and from the dI/dV vs V fits is shown in Fig. 4 (b) as a function of R_N . In our samples, the nanowire works as a rigid coherent scatterer and the tunneling process involves a transfer of an electron from one film electrode to the other through the wire acting as a complex barrier. The effective capacitance of the structure is the capacitance between two film electrodes located on the opposite sides of the wire. It appears that the portion of the electrodes that contribute to the capacitance is determined by a “horizon” [23, 27], which occurs some distance away from the wire. The schematic picture of the film electrode pattern for our structure is given in Ref. [2]. To estimate its capacitance we used equations given in Ref. [28] and the program FASTCAP [29]. The charging energies for two limited cases are shown in Fig. 4 (b) as dashed lines. The upper limit, $E_C \approx 80$ μeV , corresponds to the capacitance of the narrow film strip ($10 \mu\text{m}$ in width and $50 \mu\text{m}$ in length) directly connected to the wire. The lower limit, $8 \mu\text{eV}$, is obtained when we take into account whole pattern with contact pads which is about 3 mm in size. Most of the values of E_c extracted from the experiment fall between these two limits.

The variation of the effective charge extracted from the $G_0/(G_0 - G(T))$ dependencies is show in Fig. 4 (c) vs.

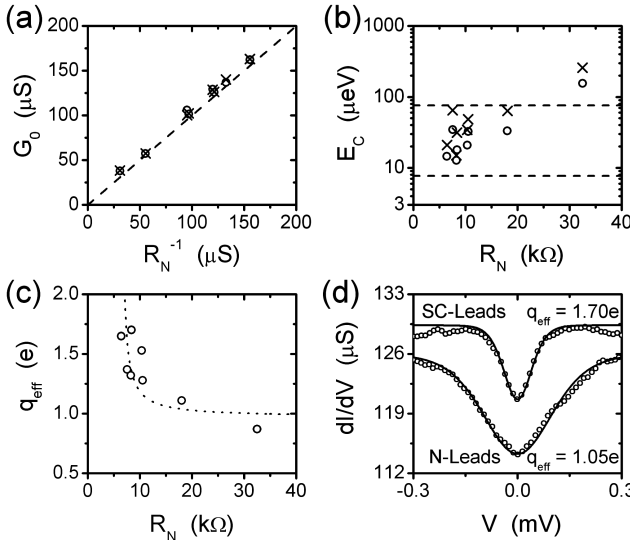


FIG. 4: (a) Values of G_0 , extracted from the GZ theory fits, plotted versus inverse R_N . Symbols are G_0 obtained from temperature dependent (\times) and voltage dependent (\circ) data. The dashed line is $G_0 = R_N^{-1}$. (b) Charging energies extracted from fits to the GZ theory and plotted versus R_N . Symbols are E_C obtained from the temperature dependent (\times) and voltage dependent (\circ) data. Dashed lines indicate the range of E_C estimated for our electrodes. (c) The effective charge extracted from dI/dV fits (Fig. 3) as a function of R_N . The dotted line is a guide to the eye. (d) Differential conductance vs. bias voltage for sample D at two different magnetic fields. At zero field the leads are superconducting (SC-Leads) and $q_{eff} = 1.70e$ whereas at high field ($B = 9$ T) the leads are driven normal (N-Leads) and q_{eff} drops to $1.05e$. Solid lines are fits to the GZ theory.

R_N . As R_N approaches the SIT critical point, which is $\simeq 6.5$ k Ω for this group of wires [2, 3, 10, 11, 12], form the insulating side, q_{eff} increases up to $\approx 2e$. This resembles the $e \rightarrow 2e$ transition observed in superconducting single-electron transistors [30]. Finally, when a perpendicular magnetic field is used to drive the electrodes normal, q_{eff} drops to $\approx e$, providing evidence that the high effective charge is due to the superconducting electrodes [Fig. 4(d)].

In summary, we have measured the conductance of MoGe nanowires and find two distinct phases: true superconductor and Coulomb insulator. Nanowires on the superconducting side of the SIT follow the LAMH theory, even for samples close to the SIT critical point. The temperature dependent and voltage dependent data of nanowires on the insulating side of the transition agree well with the predictions of the theory of dynamic Coulomb blockade for coherent diffusive wires.

We thank R. Dinsmore for providing assistance with sample fabrication. This work is supported by NSF CAREER Grant No. DMR 01-34770, DOE grant DEFG02-91-ER45439, and the Alfred P. Sloan Foundation. Fabrication was performed at CMM-UIUC supported in part by DOE grant DEFG02-91-ER45439.

[*] These authors contributed equally to this work.

- [1] F. Sharifi, A.V. Herzog, and R.C. Dynes, Phys. Rev. Lett. **71**, 428 (1993).
- [2] A. Bezryadin, C.N. Lau, and M. Tinkham, Nature **404**, 971 (1999).
- [3] A.T. Bollinger, A. Rogachev, M. Rimeka, and A. Bezryadin, Phys. Rev. B **69**, 180503(R) (2004).
- [4] A. Rogachev and A. Bezryadin, Appl. Phys. Lett. **83**, 512 (2003).
- [5] C.N. Lau, N. Markovic, M. Bockrath, A. Bezryadin, and M. Tinkham, Phys. Rev. Lett. **87**, 217003 (2001).
- [6] Y. Oreg and A.M. Finkel'stein, Phys. Rev. Lett. **83**, 191 (1999).
- [7] N. Giordano, Phys. Rev. Lett. **61**, 2137 (1988).
- [8] A.D. Zaikin, D.S. Golubev, A. van Otterlo, and G.T. Zimanyi, Phys. Rev. Lett. **78**, 1552 (1997).
- [9] D.S. Golubev and A.D. Zaikin, Phys. Rev. B **64**, 014504 (2001).
- [10] S. Klebnikov and L. P. Pryadko, Phys. Rev. Lett. **95**, 107007 (2005); S. Khlebnikov, *ibid.* **93**, 090403 (2004).
- [11] G. Refael, E. Demler, Y. Oreg, and D. S. Fisher, Phys. Rev. B **68**, 214515 (2003); G. Refael *et al.*, cond-mat/0511212.
- [12] H.P. Büchler, V.B. Geshkenbein, and G. Blatter, Phys. Rev. Lett. **92**, 067007 (2004).
- [13] S. Sachdev, P. Werner, and M. Troyer, Phys. Rev. Lett. **92**, 237003 (2004).
- [14] A. Rogachev, A.T. Bollinger, and A. Bezryadin, Phys. Rev. Lett. **94**, 017004 (2005).
- [15] M. Tian *et al.*, Phys. Rev. B **71**, 104521 (2005); M. Zgirski, K. Riikonen, V. Touboltsev, and K. Arutyunov, Nano Lett. **5**, 1029 (2005).
- [16] Y.V. Nazarov, Phys. Rev. Lett. **82**, 1245 (1999).
- [17] D.S. Golubev and A.D. Zaikin, Phys. Rev. Lett. **86**, 4887 (2001).
- [18] A. Levy Yeyati, A. Martin-Rodero, D. Esteve, and C. Urbina, Phys. Rev. Lett. **87**, 046802 (2001).
- [19] H.B. Weber, R. Häussler, H.v. Löhneysen, and J. Kroha, Phys. Rev. B, **63**, 165426 (2001); D. Beckmann, H.B. Weber, and H.v. Löhneysen, *ibid.* **70**, 033407 (2004).
- [20] J.S. Langer and V. Ambegaokar, Phys. Rev. **164**, 498 (1967); D.E. McCumber and B.I. Halperin, Phys. Rev. B **1**, 1054, (1970).
- [21] M. Tinkham, *Introduction to Superconductivity*, (McGraw-Hill, New York, 1996), 2nd ed.
- [22] J.S. Penttilä *et al.*, Phys. Rev. Lett. **82**, 1004 (1999).
- [23] J.P. Kauppinen and J.P. Pekola, Phys. Rev. Lett. **77**, 3889 (1996).
- [24] P. Joyez and D. Esteve, Phys. Rev. B **56**, 1848 (1997).
- [25] P. Joyez, D. Esteve and M.H. Devoret, Phys. Rev. Lett. **80**, 3889 (1998).
- [26] A. LevyYayati, J.C. Cuevas, and A. Martin-Rodero, Phys. Rev. Lett. **95**, 056804 (2005).
- [27] A.N. Cleland, J.M. Schmidt, and J. Clarke, Phys. Rev. Lett. **64**, 1565 (1990).
- [28] Y. Song, J. Appl. Phys. **47**, 2651 (1976).
- [29] <http://www.fastfieldsolvers.com>

[30] M.T. Tuominen, J.M. Hergenrother, T.S. Tighe, and M. Tinkham, Phys. Rev. Lett. **69**, 1997 (1992); M.T. Eiles, J. M. Martinis, and M. H. Devoret, *ibid.* **70**, 1862 (1993).